MEDWIN PUBLISHERS
Committed to Create Value for Researchers

Nanomedicine & Nanotechnology Open Access
ISSN: 2574-187X

High-Efficiency Solar Cells with a Planar Nanostructure Junction

K Sambasiva Rao[1] and Lucky Agarwal[2]*

[1]Department of Electronics & Communication Engineering, Madanapalle Institute of Technology & Science, India

[2]School of Electronics Engineering, Vellore Institute of Technology & Science, India

***Corresponding author:** Lucky Agarwal, School of Electronics Engineering, Vellore Institute of Technology & Science, Chennai, Tamil Nadu, 600127, India, Email: rel1408@mnnit.ac.in

Research Article
Volume 5 Issue 3
Received Date: October 28, 2020
Published Date: November 13, 2020
DOI: 10.23880/nnoa-16000202

Abstract

Considering the current research interest in Organic / Inorganic (ZnO) hybrid solar cells structures in developing advanced photovoltaic devices, three different types of solar cell structures are proposed. In the proposed structures, hybrid solar cell composed of ZnO nanoparticles are used as an electron-acceptor material and PEDOT:PSS is intruded in between the nanoparticles, which reported to possesses power-conversion efficiency in excess of 8%. The use of p-ZnO layer results to improve the device performance on the rigid substrate. The power-conversion efficiency of the developed solar cell was found to be as high as 10% when measured under AM 1.5G illumination. Further, simulations have been carried out whose results are in line with experimental results.

Keywords: p-n Homojunction; Hybrid Solar Cell; Photovoltaic Effect; PEDOT: PSS

Introduction

Since its inception in the year 1940, silicon (Si) solar cells have been recognized as the potential photovoltaic systems for large-scale electricity production [1,2]. The characteristic of silicon solar is the function of high-quality silicon materials which is expensive and tiresome to grow. Hence, efforts were focused on the development of comparatively economical materials for solar cells. Thin film-based solar cells are alternative and also cost-effective in comparison to the Si-based solar cells [3]. The thin-film-based inorganic solar cells are limited by tedious fabrication procedures i.e. elevated temperatures, high vacuum, numerous lithographic steps and high costs [4]. Therefore, organic thin-film solar cells have been widely investigated by researchers. There is another effective and cost-efficient category of thin-film solar cell that combines attractive properties of inorganic and organic thin-film solar cells which are known as hybrid thin-film solar cell structures [5]. These structures have higher solar power conversion efficiency along with the smart film-forming properties of conjugated polymers [6].

In the present article, the concept of ZnO based p-n homojunction has been used in conjunction with organic material to produce hybrid solar cells. This method is economical, eco-friendly and can be operated at low temperatures. Poly (3,4-ethylene dioxythiophene): poly(styrene-sulfonate) (PEDOT: PSS) has been used as the organic layer in the proposed hybrid solar cell structure. PEDOT: PSS, has the characteristics of electron blocking and whole transportation which is well reported in the most studied polymers [7]. It acts as a barrier to oxygen and as a planarizing layer to inhibit electrical shorts, and further, it improves the device lifetime. Moreover, PEDOT: PSS is acquiescent to solution-based processes which exhibits good conductivity variations (up to 1000 S/cm), work function (in the range of 4.8–5.2 eV), and high transparency in the visible region [8-10]. Aspiring to advance, the performance of the ZnO/PEDOT: PSS hybrid solar cells to the theoretical boundary [11], a series of research activities have been carried out by coating the anti-transmission (AT) layer [7,12-15], It is reported that the addition of AT layer appears to be an optimal solution to improve the PCE of ZnO/PEDOT: PSS hybrid cells [16,17] which increases the reflection and reduces the transmission. As a result, large amount of light will reach the absorber layers resulting more short-circuit current density (Jsc). However, distinct proposals were proposed at the rear side of the hybrid solar cells to proficiently collect the photo-generated carriers related to the incident light. Further, a p-Si thin film based anti-transmission (AT) layer has been proposed. The hybrid effect existing between PEDOT: PSS and p-n homojunction ZnO has been investigated and confirmed by the increased photocurrent density. To validate, experimental results of hybrid solar cell structures, numerical simulations have been carried out by using software, SILVACO ATLAS™. To simulate the I-V characteristic of the hybrid solar cells structures, single exciton dislocation model has been considered.

Fabrication of Hybrids Solar Cells

Initially, ITO coated glass of size 2x2 cm^2 were cleaned with diluted NaOH solution and successively rinsed with deionized water. Then n-ZnO nanostructure was grown on ITO coated glass substrates using an RF /DC sputtering system (AGILENT). A sintered ZnO target with the high purity of 99.99% was used for the same. RF sputtering was performed at the substrate temperature of 300°C in Ar and O_2 ambiance. The Ar and O_2 flow rate was 30 sccm, and 5 sccm, respectively. To obtain ZnO nanostructures, the total pressure was maintained at 0.5 Pa. All the films were deposited with a target-substrate distance of 80 mm and a sputtering power of 150 W. Further p-ZnO /n-ZnO homojunction has been fabricated on ITO-coated glass by a sol-gel spin coating process. The p-ZnO sol has been prepared by doping of 5 mol % Cu in ZnO [18]. The rotation speed was set to 2000 rpm for 30 sec. After wards, the PEDOT: PSS solution prepared in chloroform was spin-coated on the grown p-n homojunction at the spinning speed of 5000 rpm for 60 s. Afterwards; the samples were heated on a hotplate at 100°C for 10 minutes to evaporate the residue. Next, a 50 nm thick p-Si layer has been introduced by RF magnetron sputtering in the same environmental condition as mentioned above. At last, a 50-nm thick Pd electrode was deposited on the surface of the p-Si layer via thermal vacuum coating unit (Agilent). In the vacuum coating current has been increased slowly from 0 a to 1 KA. Following aforementioned methodology three structures have been fabricated for hybrid solar cell i.e. Pd/ p-Si/ PEDOT: PSS/ p-ZnO/ n-ZnO/ ITO, Pd/ PEDOT: PSS/ p-ZnO/ n-ZnO/ ITO and Pd/ PEDOT: PSS/ n-ZnO/ ITO.

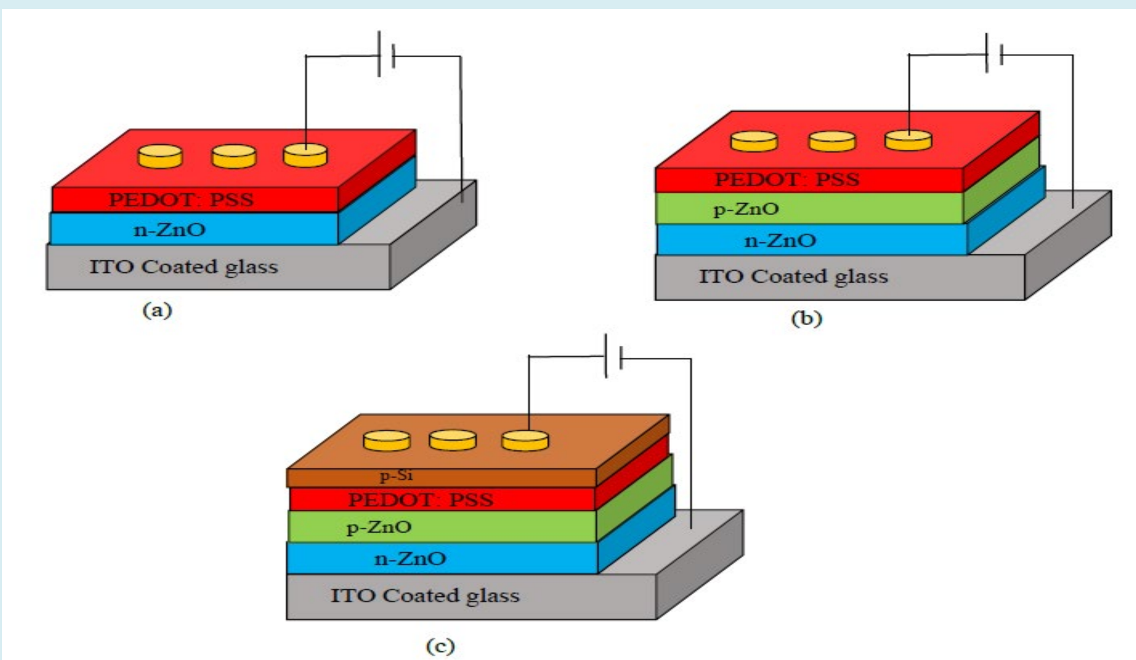

Figure 1: Schematic diagram of fabricated (a) Pd/ PEDOT: PSS/ n-ZnO/ ITO, (b) Pd/ PEDOT: PSS/ p-ZnO/n-ZnO/ ITO, and (c) Pd/ p-Si/ PEDOT: PSS/ p-ZnO/ n-ZnO/ ITO Hybrid solar cell.

Copyright© K Sambasiva Rao and Lucky Agarwal.

The thickness of the deposited thin films, refractive index (η), extinction coefficient (k) and reflectivity of p-Si AT layer were measured by spectroscopic ellipsometry (J.A. Woollam M-2000 DI) in the wavelength range of 300–800 nm. Further, the current density-voltage (J-V) characteristics of the hybrid solar cells have been measured on four probe measurement system using semiconductor parameter analyzer (Keithley 2400 digital source meter). All the experimental measurements have been carried out under the simulated sunlight of varying intensity with illumination provided by a xenon lamp (Oriel) and AM 1.5 filter. The open area of the cells has 1.5 cm × 1.5 cm, whereas the area covered with Pd electrodes has 0.25 cm^2. The Xenon light source with a spot size of 3.0 × 3.0 mm has been used to measure the EQE value. The schematic of the fabricated three solar cell structures has been shown in the Figure 1(a, b, c).

Result and Discussion

This section shows the results obtained for the prepared hybrid solar cell structures. The prepared solar cell possesses structure Pd/ PEDOT: PSS/ n-ZnO/ ITO in which the PEDOT: PSS layer act as an electron blocking layer, n-ZnO nanostructures behaves as the active layer, palladium (Pd) electrode work as device contacts and ITO coated glass act as a bottom contact and substrate. The fabricated cell demonstrates promising photovoltaic performance, with an open-circuit voltage VOC = 0.501 V, short-circuit current JSC = 18.27 mA cm^{-2}, and fill factor (FF) =31, corresponding to PCE 2.17% under standard Sun AM 1.5 simulated solar irradiation. However, the conductivity of PEDOT:PSS is low and to overcome this limitation the p-ZnO has been introduced to form p-n homojunction in order to achieve better photoresponse under U-V illumination [19]. The modified resulting structure is Pd/ PEDOT: PSS/p-ZnO/ n-ZnO/ ITO as shown in figure 1b. On introducing p-ZnO between PEDOT: PSS and n-ZnO layer enhances the VOC 0.532 V, JSC 23.72 mA cm^{-2}, and FF 41, correspondingly PCE raise to 5.39%. Deposition of p-Si layer on PEDOT: PSS layer further increases the VOC, JSC, FF, and PCE to 0.568 V, 35.62 mA cm^{-2}, 45 and 8.08%, respectively. The increases in electrical parameters are due to the fact that the p-Si has high reflectivity that reduces the photon loss and sustains light within the p-n junction that further elevates the efficiency of the hybrid solar cell.

The estimated thickness of the PEDOT: PSS thin film in the solar cell structures was ~50 nm. The reflection spectrum of p-Si deposited on p-n junction in structure Pd/ p-Si/ PEDOT: PSS/ p-ZnO/ n-ZnO/ ITO was tested using ellipsometry as shown in Figure 2a. It can be observed that p-Si displays higher reflectivity, especially in the ultraviolet region. Figure 2b illustrates the absorption spectrum of PEDOT: PSS layer in structures Pd/ p-Si/ PEDOT: PSS/ p-ZnO/ n-ZnO/ ITO, Pd/ PEDOT: PSS/ p-ZnO/ n-ZnO/ ITO and Pd/ PEDOT: PSS/ n-ZnO/ ITO. It is obvious from the spectrum that the layer of PEDOT: PSS have small parasitic absorptions centered at 550 nm. It can be observed that p-Si displays higher reflectivity, especially in the ultraviolet band.

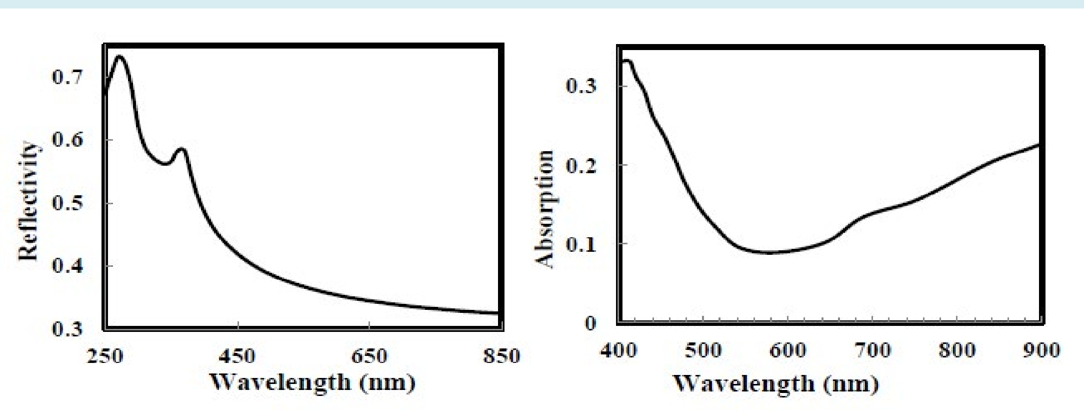

Figure 2: (a) Reflection spectrum of p-Si and (b) absorption spectrum of PEDOT: PSS layer in structure.
PEDOT: PSS and p-Si layer show small absorption indicating small current loss caused by the absorption of photons in the fabricated three solar cell structures.

Figures 3(a) and 3(b) shows the experimental and simulated current–voltage (J–V) characteristics of the proposed structures i.e. Pd/ p-Si/ PEDOT: PSS/ p-ZnO/ n-ZnO/ ITO, Pd/ PEDOT: PSS/ p-ZnO/ n-ZnO/ ITO and Pd/ PEDOT: PSS/ n-ZnO/ ITO. The value of, Jsc, Voc, fill factor (FF) and PCE were estimated from Figure 3. found to be 0.568 V, 35.62 mA/cm^2, 45, and 8.08% respectively for Pd/ p-Si/ PEDOT: PSS/ p-ZnO/ n-ZnO/ ITO solar cell. The simulated

Copyright© K Sambasiva Rao and Lucky Agarwal.

structure of the aforementioned solar cell gives PCE of 13.9 %. As it can be observed from Figure 3 (b) that the simulation results have showed good agreement with the experimental results. The performance parameters of the proposed solar cells with different structures have been compared in the Table 1.

Devices		Voc(V)	Vm(V)	Jsc (mA/cm2)	Jm (mA/cm2)	FF (%)	Efficiency (%)
ITO/n-ZnO/ PEDOT:PSS/Pd	Simulated	0.49	0.4218	19.7	11.29	57	5.5
	Experimental	0.501	0.21	18.27	16.27	31	2.17
ITO/n-ZnO/p-ZnO/Pedot:PSS/Pd	Simulated	0.548	0.456	24.5	18.35	62	8.32
	Experimental	0.532	0.235	23.72	22.1	41	5.39
ITO/n-ZnO/p-ZnO/Pedot:PSS/ p-	Simulated	0.575	0.49	36.8	28.2	66	13.9
	Experimental	0.568	0.319	35.62	30.87	45	8.08

Table 1: Simulated and experimental parameters evaluated for different solar structures.

The maximum power point (MPP) of the fabricated ~~a~~ solar cell is situated close to the bend in the J-V curve as shown in figure 3. Parameters i.e. maximum voltage (Vmp) and maximum current (Imp) have been obtained from the open circuit voltage and the short circuit current for the given solar cell structure under consideration. Both simulation and experimental parameters obtained from different solar cell structures have been summarized in the Table 1.

The introduction of a p-n junction between the PEDOT: PSS and ITO electrode may bring an effective back surface field that efficiently suppresses the recombination rate at the rear surface via a downward band bending. The introduction of the homojunction may thus lead to the better use of the photon-generated carrier. The simulated results are found to be in line with the experimental results trends. The difference between them may be accounted due to the surface recombination at the ITO and low shunt resistance.

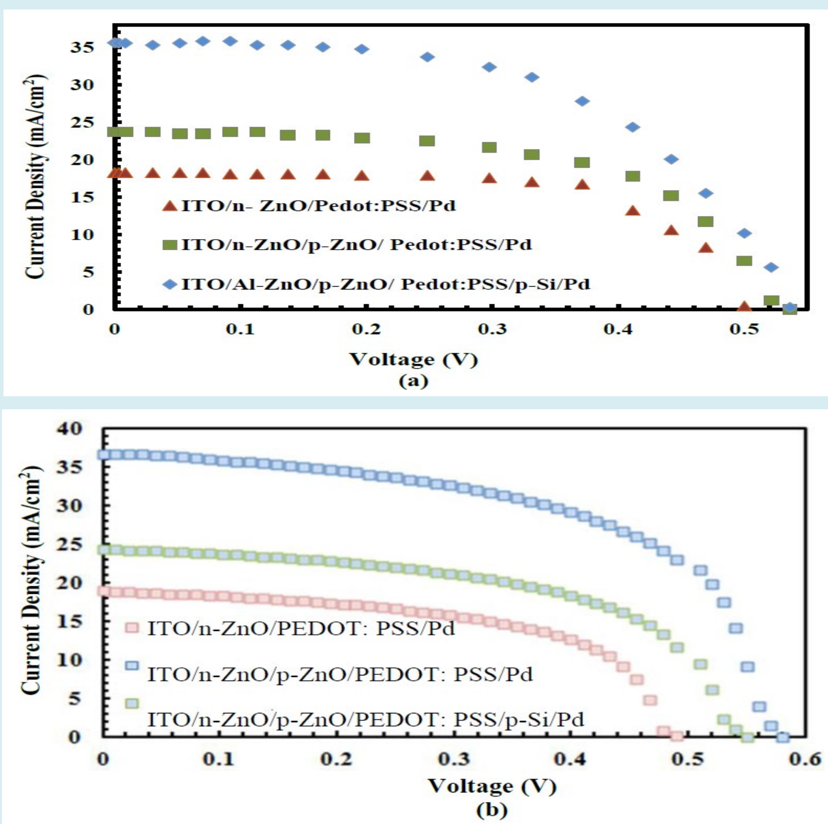

Figure 3: J-V characteristics of three fabricated solar cells (a) experimental and (b) simulated results.

Copyright© K Sambasiva Rao and Lucky Agarwal.

A comparison between Pd/ PEDOT: PSS/ n-ZnO/ ITO, and the Pd/ PEDOT: PSS/ p-ZnO/ n-ZnO/ ITO homojunctions showed improved values of Voc, Jsc, and PCE as 0.532 mV, 23.72 mA/cm^2, and 5.39%, respectively. Further ~~by~~ the values of simulation, the Voc, Jsc, and PCE are 0.548 mV, 24.5 mA/cm^2, and 8.32 % respectively were estimated by simulation. In the literature, it is reported that the efficiency of solar cells can further be improved by introducing the reflector layer between the front electrode, i.e., Pd and PEDOT: PSS. This sandwich structure confines the photons within the homojunction. A p-Si layer has been used as the reflector due to high reflectance as shown in Figure 2 (b). So in comparison of Pd/ PEDOT: PSS/ p-ZnO/ n-ZnO/ ITO, the introduction of p-Si layer in Pd/ p-Si/ PEDOT: PSS/ p-ZnO/ n-ZnO/ ITO solar cell structure overcame the photon loss problem, which can be observed from the energy band diagram of the proposed solar cell in Figure 04. From Figure 4, it can be observed that the value of lowest and the highest occupied molecular orbital energies are – 4.35 eV and –7.7 eV for of ZnO, whereas for p-ZnO these values are –4.4 eV and –7.3 eV respectively [13,20,21]. As a result, when a thin layer of p-ZnO was deposited in contact with n-ZnO to form p-n homojunction p-ZnO act as an ideal “electron acceptor” for p-n homojunction that creates a donor–acceptor planar homojunction system as illustrated in Figure 1. Under the irradiation from the solar simulator (AM 1.5), excitons are generated by the absorption of light in the n- ZnO layer. The oppositely charged holes and electrons in excitons are then separated at the donor-acceptor interface, which is shown in Figure 4.

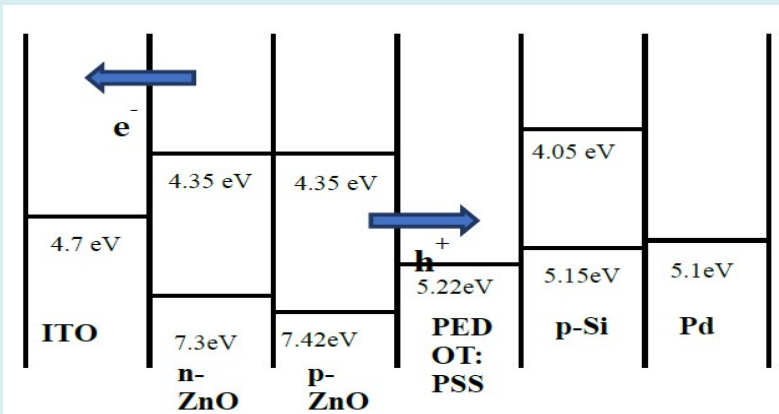

Figure 4: Band Structure of the proposed solar cell.

The average Jsc of the structure Pd/ p-Si/ PEDOT: PSS/ p-ZnO/ n-ZnO/ ITO is 30.87 mA/cm^2, demonstrating increase of 47% and 28.4 % in comparison with the Pd/ PEDOT: PSS/ n-ZnO/ ITO and Pd/ PEDOT: PSS/ p-ZnO/ n-ZnO/ ITO solar cell structures. The estimated value of Jsc was found to be 28.2 mA/cm^2 is much lower than the theoretically simulated value of Jsc 36.8 mA/cm^2. The difference in current density has been accounted due to the recombination that occurred on the surface or in bulk, due to which the carrier density has been reduced, causing the decrease of short-circuit current density.

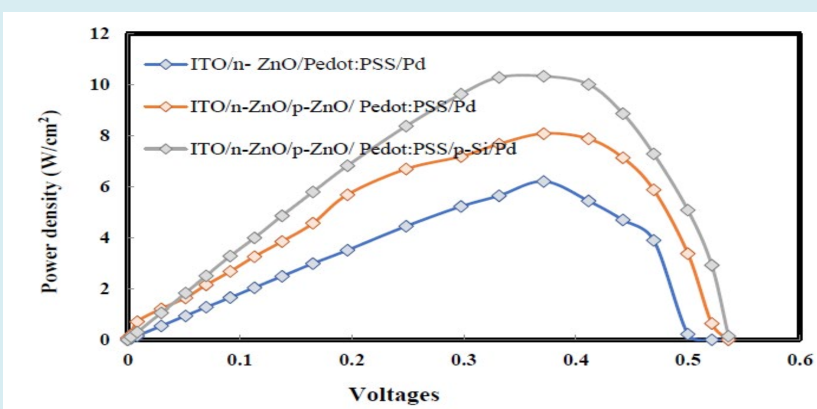

Figure 5: The power density versus voltage characteristics of different solar cells.

Copyright© K Sambasiva Rao and Lucky Agarwal.

The power delivered by a solar cell is the product of voltage (Vmp) and current (Imp) at Maximum Power Point (MPP). Figure 5 shows the power density (units) versus voltage curve for the three fabricated three different solar cell structures. If the multiplication is carried out, point to point, for all voltages from short-circuiting to open-circuit conditions, the power curve is obtained for a given radiation level. Figure 5 shows the power density (units) versus voltage curve for the three fabricated three different solar cell structures.

The external quantum efficiency (EQE) (indicative of photon to electron conversion) [22,23] of prepared solar cell structure has also been measured which is shown in Figure 6. As anticipated, the cells with the p-Si as reflector layer, exhibited a larger EQE value of greater than 68% in the visible regions in comparison with the Pd/ PEDOT: PSS/ p-ZnO/ n-ZnO/ ITO and Pd/ p-Si/ PEDOT: PSS / n-ZnO/ ITO solar cell structure. It may be due to the increased amount of the incident light that reaches to the p-n junction due to the presence of p-Si anti-transmission layer. In the ultraviolet band, the unexpected lower EQE for all the three solar cell structure is expected due to the parasitic absorption of PEDOT: PSS layer.

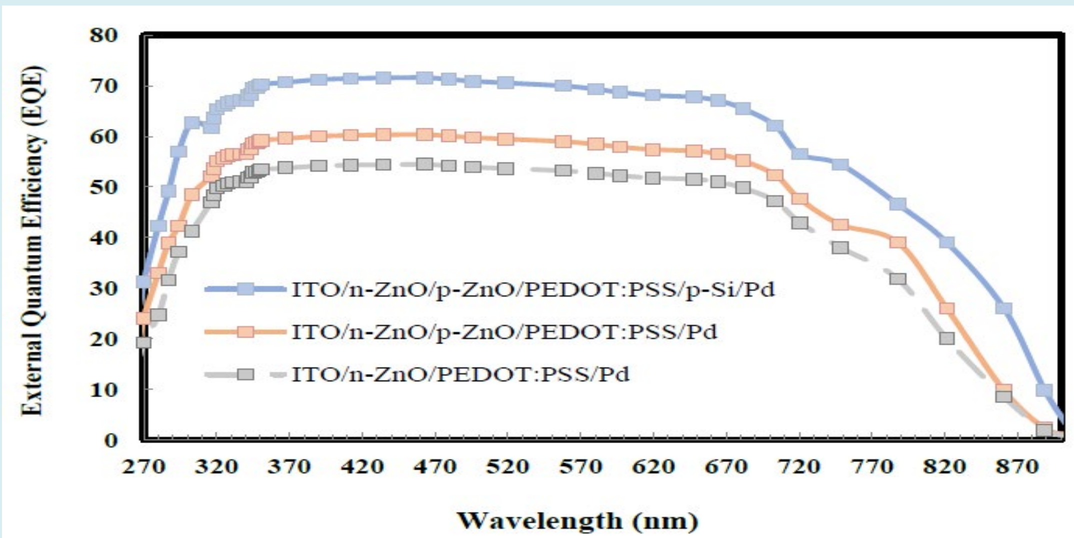

Figure 6: External quantum efficiency of the three fabricated solar cell structures.

The fabricated devices stability has been examined for one year in an interval of 45 days. It was found that Voc showed the highest consistency in reproducibility with a value of 0.59 eV and short-circuit current density (Jsc) as 35.7 mA/ cm^2 for the proposed solar cell with homojunction and p-Si. The combination of such parameters with the best-evaluated fill factors (70%) yields a simulated and experimental PCE of 13.7% and 8.1 %, respectively. Such a high reproducibility of the fabricated solar cells and the better PCEs reveal the potential of fabricated structure. From the above results, it can be observed that the mesoporous scaffolds utilized in the device architectures are superfluous for the production of high-performance cells [24,25].

Conclusion

In this article, the fabrication, experimentation and simulation of the three different solar cell structures have been carried out and their performances were compared. The average Jsc of the Pd/ p-Si/ PEDOT: PSS/ p-ZnO/ n-ZnO/ ITO solar cell was estimated to be 30.87 mA/cm^2, demonstrating an increase by factor of 47% and 28.4 % in comparison with the structure Pd/ PEDOT: PSS/ n-ZnO/ ITO and Pd/ PEDOT: PSS/ p-ZnO/ n-ZnO/ ITO solar cell. It is also found that out of the three different structures the Pd/ p-Si/ PEDOT: PSS/ p-ZnO/ n-ZnO/ ITO structure showed much improved performance in terms of efficiency 8.08 %. This is due to the fact that the introduction of p-n homojunction and the p-Si reflector increases the Voc, Jsc, and PCE parameter. Further, to validate the experimental results, model-based studies has been carried out on software SILVACO ATLAS™ for three different solar structures. Theoretical and simulation results also reveal that Pd/ p-Si/ PEDOT: PSS/ p-ZnO/ n-ZnO/ ITO solar cell structure has showed the highest efficiency (13.9 %) than other structures. Therefore, model results are in line with experimental which has showed more confidence about proposed structure. Further, the structure has been tested for every 45 days, in a year which showed good repeatability.

Copyright© K Sambasiva Rao and Lucky Agarwal.

Acknowledgement

The authors are grateful to CIR MNNIT Allahabad for providing the fabrication facilities and IIT Kanpur for providing the characterization facilities.

Conflict of Interest Statement

No Conflict of Interest Statement

References

1. Kroon J, Hinsch A (2003) Dye-sensitized solar cells. Organic Photovoltaics, Springer, pp: 273-290.
2. Cheng Y, Qing Dan Yang, Jingyang Xiao, Qifan Xue, Ho Wa Li, et al. (2015) Decomposition of organometal halide perovskite films on zinc oxide nanoparticles. ACS applied materials & interfaces 7(36): 19986-19993.
3. Shah A, Torres P, Tscharner R, Wyrsch N, Keppner H (1999) Photovoltaic technology: the case for thin-film solar cells. Science 285(5428): 692-698.
4. Huynh WU, Dittmer JJ, Alivisatos AP (2002) Hybrid nanorod-polymer solar cells. Science 295(5564): 2425-2427.
5. Conings B, Baeten L, De Dobbelaere C, D'Haen J, Manca J, et al. (2014) Perovskite-based hybrid solar cells exceeding 10% efficiency with high reproducibility using a thin film sandwich approach. Adv Mater 26(13): 2041-2046.
6. Park KT, Kim HJ, Park MJ, Jeong JH, Lee J, et al. (2015) 13.2% efficiency Si nanowire/PEDOT:PSS hybrid solar cell using a transfer-imprinted Au mesh electrode. Sci Rep 5(1): 12093.
7. Yang Z, Fang Z, Sheng J, Ling Z, Liu Z (2017) Optoelectronic Evaluation and Loss Analysis of PEDOT:PSS/Si Hybrid Heterojunction Solar Cells. Nanoscale Res Lett 12(1): 26.
8. Lee BR, Kim J, Kang D, Lee DW, Ko SJ, et al. (2012) Highly efficient polymer light-emitting diodes using graphene oxide as a hole transport layer. ACS Nano 6(4): 2984-2991.
9. Wei WR, Tsai ML, Ho ST, Tai SH, Ho CR, et al. (2013) Above-11%-efficiency organic-inorganic hybrid solar cells with omnidirectional harvesting characteristics by employing hierarchical photon-trapping structures. Nano Lett 13(8): 3658-3663.
10. Alemu D, Wei HY, Ho KC, Chu CW (2012) Highly conductive PEDOT: PSS electrode by simple film treatment with methanol for ITO-free polymer solar cells. Energy Environ Sci 5(11): 9662-9671.
11. Rawat G, Somvanshi D, Kumar H, Kumar Y, Kumar C, et al (2015) Ultraviolet detection properties of p-Si/n-TiO 2 heterojunction photodiodes grown by electron-beam evaporation and sol–gel methods: A comparative study. IEEE Transactions on Nanotechnology 15(2): 193-200.
12. Wang M, Li S, Zhang P, Wang Y, Li H, et al. (2015) A modified sequential method used to prepare high quality perovskite on ZnO nanorods. Chem Phys Lett 639: 283-288.
13. Zhang X, Zhang X, Yang D, Yang Z, Guo X, et al. (2016) Improved PEDOT:PSS/c-Si hybrid solar cell using inverted structure and effective passivation. Sci Rep 6(1): 35091.
14. Zhang T, Zhang P, Li S, Li W, Wu Z, et al. (2013) Black silicon with self-cleaning surface prepared by wetting processes. Nanoscale Res Lett 8(1): 351.
15. Li H, Li S, Wang Y, Sarvari H, Zhang P, et al. (2016) A modified sequential deposition method for fabrication of perovskite solar cells. Sol Energy 126: 243-251.
16. Thomas JP, Srivastava S, Zhao L (2015) Reversible structural transformation and enhanced performance of PEDOT: PSS-based hybrid solar cells driven by light intensity. ACS Appl Mater Interfaces 7(14): 7466-7470.
17. Sun Y, Yang Z, Gao P, He J, Yang X, et al. (2016) Si/PEDOT:PSS Hybrid Solar Cells with Advanced Antireflection and Back Surface Field Designs. Nanoscale Res Lett 11(1): 356.
18. Agarwal L, Singh BK, Tripathi S, Chakrabarti P (2016) Fabrication and characterization of Pd/cu doped ZnO/Si and Ni/cu doped ZnO/Si Schottky diodes. Thin Solid Films 612: 259-266.
19. Pudasaini PR, Ruiz Zepeda F, Sharma M, Elam D, Ponce A, et al. (2013) High efficiency hybrid silicon nanopillar-polymer solar cells. ACS Appl Mater Interfaces 5(19): 9620-9627.
20. Guo W (2010) Epitaxial growth and properties of zinc oxide thin films on silicon substrates. University of Michigan.
21. Qi B, Wang J (2012) Open-circuit voltage in organic

Copyright© K Sambasiva Rao and Lucky Agarwal.

solar cells. J Mater Chem 22(46): 24315-24325.

22. Green MA, Emery K, Hishikawa Y, Warta W, Dunlop ED (2015) Solar cell efficiency tables (Version 45). Prog photovoltaics Res Appl 23(1): 1-9.

23. Menglin Li, Xiuwen Xu, Yuemin Xie, Ho Wa Li, Yuhui Ma, et al. (2019) Improving the conductivity of sol–gel derived NiO x with a mixed oxide composite to realize over 80% fill factor in inverted planar perovskite solar cells. Journal of materials chemistry A 7(16): 9578-9586.

24. Liu D, Kelly TL (2013) Perovskite solar cells with a planar heterojunction structure prepared using room-temperature solution processing techniques. Nat Photonics 8(2): 133-138.

25. Cheng Y, Menglin L, Xixia L, Cheung SH, Chandran HT, et al. (2019) Impact of surface dipole in NiOx on the crystallization and photovoltaic performance of organometal halide perovskite solar cells. Nano Energy 61(7): 496-504.

Copyright© K Sambasiva Rao and Lucky Agarwal.